

Lawrence Berkeley National Laboratory

Recent Work

Title

PROGRAM PLAN FOR THE MBE-4 MULTIPLE BEAM EXPERIMENT

Permalink

<https://escholarship.org/uc/item/4hc6p94r>

Author

Avery, R.T.

Publication Date

1985-02-01



Lawrence Berkeley Laboratory

UNIVERSITY OF CALIFORNIA

RECEIVED
FEB 10 1985
LIBRARY AND DOCUMENTS SECTION

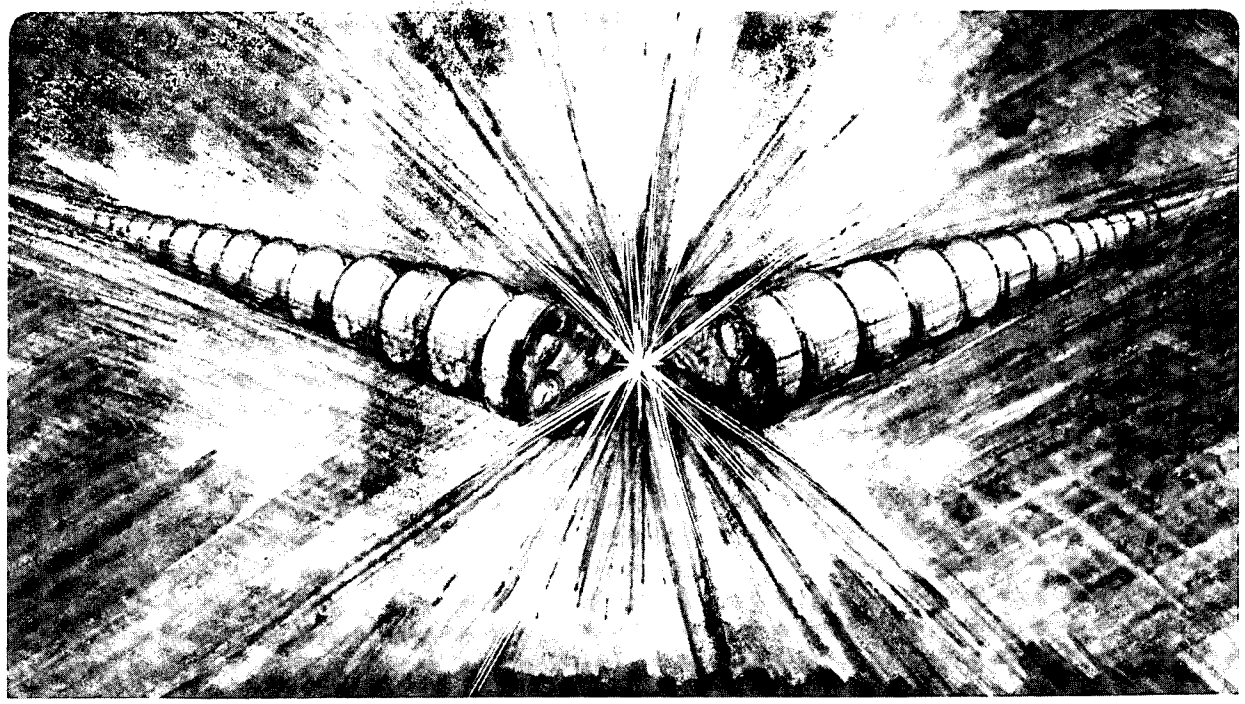
Accelerator & Fusion Research Division

PROGRAM PLAN FOR THE MBE-4 MULTIPLE BEAM EXPERIMENT

R.T. Avery

February 1985

TWO-WEEK LOAN COPY
*This is a Library Circulating Copy
which may be borrowed for two weeks.*



LBL-19592
c.2

DISCLAIMER

This document was prepared as an account of work sponsored by the United States Government. While this document is believed to contain correct information, neither the United States Government nor any agency thereof, nor the Regents of the University of California, nor any of their employees, makes any warranty, express or implied, or assumes any legal responsibility for the accuracy, completeness, or usefulness of any information, apparatus, product, or process disclosed, or represents that its use would not infringe privately owned rights. Reference herein to any specific commercial product, process, or service by its trade name, trademark, manufacturer, or otherwise, does not necessarily constitute or imply its endorsement, recommendation, or favoring by the United States Government or any agency thereof, or the Regents of the University of California. The views and opinions of authors expressed herein do not necessarily state or reflect those of the United States Government or any agency thereof or the Regents of the University of California.

PROGRAM PLAN FOR
THE MBE-4 MULTIPLE BEAM EXPERIMENT*

Prepared by
Robert T. Avery
on behalf of the

Heavy Ion Fusion Accelerator Research Group
Accelerator and Fusion Research Division
Lawrence Berkeley Laboratory

February 1985

* This work was supported by the Director, Office of Energy Research, Office of Basic Energy Sciences, U.S. Dept. of Energy, under Contract No. DE-AC03-76SF00098.

LAWRENCE BERKELEY LABORATORY
ACCELERATOR & FUSION RESEARCH DIVISION

Heavy Ion Fusion Accelerator Research (HIFAR) Group
Fiscal Year 1985

Group Leader: D. Keefe
Deputy Leader: T. Fessenden

Scientific Staff: J. Bisognano, V. Brady, C. Celata,
W. Chupp, T. Fessenden, D. Judd, D. Keefe,
C. Kim, G. Krafft, L. Laslett, E. Lee,
L. Smith, M. Tiefenback, A. Warwick.

Engineering/Design Staff:

Mechanical: R. Avery, T. Chan, O. Fredriksson,
T. Henderson, J. Hovingh, J. Meneghetti,
J. Shkredka, D. Vanecek.

Electronics: D. Brodzik, C. Chavis, A. Faltens, D. Gough,
E. Hartwig, E. Hazelton, C. Pike,
S. Rosenblum.

Technical Staff:

Mechanical: Z. Daigian, E. Edwards, W. Ghiorso,
W. Greenway, R. Hipple, (C. Kemp-Supercon),
B. MacDonnell, H. Meyer, S. Ryce, M. Towler.

Electronics: C. Houston, A. Kruser, S. Meintz, T. Purtell,
R. Rice, G. Stoker.

Administrative/Clerical Staff (Shared):

J. Kono, S. Mesetz, J. Mohrman, A. Tidwell,
O. Wong, J. Zilver.

EXECUTIVE SUMMARY

In 1981 scientists at LBL, LANL, and SLAC developed a research plan⁽¹⁾ to explore both the rf/storage ring and induction linac approaches to heavy ion inertial fusion power. Recognizing that funding for both in parallel would not be available, a more detailed 1983 plan⁽²⁾ identified a High Temperature Experiment (HTE) based on a multiple-beam induction linac as a major near term programmatic objective for the U.S. Heavy Ion Inertial Fusion program. A cost goal for the facility was set at 60-80 M\$ (FY84) with construction anticipated during FY87-FY89. The HTE will be able to develop technology at a scale adequate for an accurate fusion driver cost assessment and verify the physics of the interaction of heavy ion beams with matter by heating solid targets to temperatures of 50 to 100 eV. The linac will accelerate, for example, 16 sodium ion beams to 125 MeV at a total current of 100 A, increased to 1000 A at the target by final compression. The experiment will reach, remarkably, within a factor of three of testing at full scale many of the important features of a power plant driver.

The 1983 plan also recognized that a pilot multiple-beam accelerator that would test on a much shorter scale as many features of the HTE accelerator as possible was the logical first step toward HTE. A Multiple Beam Experiment (MBE-16) was designed^(3,4) that would test the production, acceleration, and handling of 16 parallel cesium and sodium beams at currents and energies similar to those that will exist in the front end of the HTE accelerator. These designs were presented at the DOE Review in June 1984. The sizes of the MBE-16 induction units were chosen to be of a large enough scale that they would simulate the largest units needed in HTE. Thus, this experiment was designed as a direct route to the HTE in that it would both demonstrate much of the accelerator physics and develop much of the HTE accelerator technology. During the summer of 1984, it became clear that budget appropriations required to construct the MBE-16 on a timely schedule would not be forthcoming. As a consequence, the Multiple Beam Experiment was redefined with a reduced number of beams (from 16 down to 4) and with cores of much smaller radius, and the designation was changed to MBE-4 to reflect the change to four ion beams. This is a much smaller experiment that models much of the physics of the HTE accelerator and, indeed, can provide experimental answers to accelerator physics questions earlier than could MBE-16. However, MBE-4

will do little to develop technology at the scale necessary for the HTE; the technology scale-up must await a better budgetary climate in a later fiscal year.

MBE-4

The MBE-4 experiment will use four beams of cesium at an injection energy of 0.2 MV. These beams will be accelerated to nearly 1.0 MV by 24 linear induction accelerating units. In the most aggressive acceleration schedules being contemplated, the beamlet current will increase from approximately 10 mA at injection to nearly 40 mA at the end of the experiment. Thus, the MBE-4 will demonstrate significant current amplification resulting from both an increase in particle speed and a shortening of the length of the beam bunch. Moreover, as in HTE, fields must be provided at the head and tail of the beam that prevent space charge from spreading the bunch length. In examining the scaling with injection energy, and with quadrupole size, we have been careful to preserve space charge domination of the beams, both transversely (depends on beam current density) and longitudinally (depends on line density of charge). We note that the total beam-power amplification in MBE-4 could be a factor of eighteen.

In some respects the MBE-4 is a one-tenth scale version of the MBE-16 which was described in the June 84 review. The minor transverse dimensions of the electrostatic lattice are the same as those of the MBE-16 design. However, since there are only apertures for four beams in the MBE-4 design, the major lattice diameter is reduced to less than 12 inches. A second principal difference is a reduction of the beam injection energy by a factor of ten which permits a corresponding reduction in the amount of magnetic material contained in the induction accelerator units to achieve the same ratio of output to input energy.

The technical description in subsequent chapters treats the arrangement of the Injector System (made up of an existing High Voltage Marx Generator, a new Four-beam Source array and a Beam Conditioning Unit for matching and steering) and the Accelerator Apparatus which contains the 24 shaped-pulse accelerating units. Flexibility in diagnostic capability and physics experiments has been maintained insofar as possible.

PROGRAM PLAN FOR THE MBE-4 MULTIPLE BEAM EXPERIMENT

February 1985

CONTENTS

Heavy Ion Fusion Accelerator Research (HIFAR) Group	(i)
Executive Summary	(ii)
List of Figures	(vi)
List of Tables	(viii)
A INTRODUCTION	1
B MBE-4 PRINCIPAL PERFORMANCE PARAMETERS	3
C MBE-4 GENERAL ARRANGEMENT	5
D MBE-4 INJECTOR SYSTEM	10
D1 Marx HV Generator	10
D2 Four-Beam Source	10
D3 Beam Conditioning Unit	14
D3.1 Collimating Apertures	14
D3.2 Steering Arrays	17
D3.3 Matching Quadrupoles	17
D3.4 Diagnostic Boxes	25
D3.5 Faraday Cup Array	27
D3.6 Capacitive Pickup Array	27
D3.7 Emittance Sensors	27
D3.8 Harps	32
D3.9 Support and Alignment	32
D4 Vacuum System	35
D5 Control and Monitoring	35
D6 Installation	35
E ACCELERATOR APPARATUS	40
E1 Induction Acceleration	40
E1.1 Induction Insulator	40
E1.2 Induction Cores	43
E1.3 Induction Power System	45

E2	Timing System	45
E3	Accelerator Quadrupoles	48
E4	Diagnostics	48
	E4.1 Beam Sensing Boxes	50
	E4.2 Faraday Cup Array	50
	E4.3 Emittance Sensors	50
	E4.4 Harps	50
	E4.5 Energy Analyzer	50
	E4.6 Steering Arrays	50
E5	Support and Alignment	51
E6	Vacuum System	51
E7	Control and Monitoring	52
E8	Installation	52
F	SCHEDULE	53
G	EXPERIMENTAL PROGRAM	55
	G1 Accelerator Physics Addressed by MBE-4	57
	G1.1 Effects Produced by Multiple Beams	57
	G1.2 Bunch Length Control	57
	G1.3 Induction Acceleration and Current Amplification of Ion Beams	57
	G1.4 Longitudinal Ion Beam Dynamics	57
	G1.5 Longitudinal/Transverse Coupling	58
	G1.6 6-Dimensional Emittance Growth	58
	G1.7 Beam Position Control and Steering	58
	G1.8 Reduced Voltage Injection	59
	G2 Issues Not Fully Addressed by MBE-4	59
	G2.1 Number of Pulsers	59
	G2.2 Transition to Magnetic Focussing	59
	G2.3 Fabrication and Alignment Errors	60
	G2.4 Injection Energy	60
	G2.5 Full-Scale Components	60
	G3 MBE-4 Future Modifications	60
	G3.1 Change in Lattice Period	60
	G3.2 Magnetic Quadrupoles	61
	G3.3 Additional Length	61
	G3.4 Many Low-Voltage Pulsers	61
	REFERENCES	63

LIST OF FIGURES

	<u>Page</u>
Fig. C-1	Plan View Showing MBE-4 Located in Existing Building 58. 6
Fig. C-2	Cross-Section of Building 58 Hi-Bay Looking West Showing Location of MBE-4. 7
Fig. C-3	MBE-4 Diagrammatic Layout. 8
Fig. C-4	Side View of Entire MBE-4 Apparatus. 9
Fig. D2-1	MBE-4 Injector System; Four Beam Source 11
Fig. D2-2	Ion Trajectories for One of Four Cesium Ion Beams. 13
Fig. D3-1	Tentative Locations of Diagnostic Devices 16
Fig. D3.2-1	Isometric View of Steering Array for Ion Beams 18
Fig. D3.2-2	Steering Array Electrical Power Diagram for One of Four Ion Beams. 19
Fig. D3.3-1	Transverse Cross-Section of Matching Quadrupole Array. 20
Fig. D3.3-2	Longitudinal Cross-Section of Matching Quadrupole Doublet Array. 21
Fig. D3.3-3	An Example of Quadrupole Voltages Producing Suitable Matching from the MBE-4 Injector to the Accelerator Sections. 10 mA, 200 keV Cesium Ion Beam having Emittance of $1.5 \times 10^{-7} \pi$ m-rad. 23
Fig. D3.3-4	Power Schematic for MBE-4 Quadrupole Focussing Systems. 24
Fig. D3.4-1	Transverse Cross-Section (Looking Upstream) of Diagnostic Box #M4 with Four Diagnostic Devices Installed. 26

Fig. D3.5-1	Configuration of Faraday Cup Array.	28
Fig. D3.5-2	Electrical Circuit for Faraday Cup Array and Capacitive Pickup Array.	29
Fig. D3.6-1	Configuration of Capacitive Pickup Array.	30
Fig. D3.7-1	Configuration of an Emittance Sensor Array for Measuring Emittance in One Plane.	31
Fig. D3.7-2	Electrical Circuit for an Emittance Sensor Array.	33
Fig. D3.8-1	Electrical Circuit Schematic for the Harps.	34
Fig. D4-1	MBE-4 Vacuum Schematic Injector System and First Accelerator Section.	36
Fig. D6-1	MBE-4 Phase 1A Injector Installation and Test Configuration.	38
Fig. D6-2	MBE-4 Phase 1B Installation/Test Configuration (through Box #M1).	39
Fig. E1-1	MBE-4 Induction Acceleration Diagram.	41
Fig. E1.1-1	Induction Insulator and Core Configuration.	42
Fig. E1.3-1	Examples of Theoretical and Real World Waveforms Being Considered for Incorporation into MBE-4.	46
Fig. E2-1	Electrical Circuit Schematic for the Timing System.	47
Fig. F-1	MBE-4 Schedule Objectives.	54

LIST OF TABLES

	<u>Page</u>	
Table B-1	Principal Parameters of MBE-4 Multiple Beam Experiment with Corresponding Values for MBE-16 and HTE Included for Comparison.	4
Table D2-1	MBE-4 Injector Four-Beam Source Principal Parameters.	12
Table D3-1	Diagnostic Devices in Beam Conditioning Unit.	15
Table D3.3-1	Injector System Beam Conditioning Unit Electrostatic Matching Quadrupole Array Parameters.	25
Table E1.2-1	Induction Cores and Core Material Available for Use in MBE-4	44
Table E4-1	Diagnostic Devices in MBE-4 Accelerator Apparatus	49
Table G-1	Comparison of the MBE-4 and the HTE Accelerators	56

A. INTRODUCTION

The Heavy Ion Fusion Accelerator Research (HIFAR) program⁽⁵⁾ at the Lawrence Berkeley laboratory (LBL) is a research and development effort directed towards collection of a database regarding heavy ion accelerators that could be applicable for future heavy ion inertial fusion power generation. Present HIFAR plans call for several steps leading in a few years to the construction of a High Temperature Experiment (HTE) which would produce significant heating of a target. The accelerator portion of HTE will incorporate several innovations including (a) generation of multiple high current ion beams of low emittance, (b) simultaneous induction acceleration and transport of the multiple ion beams without sacrifice of emittance, and (c) current amplification which demands shaped accelerating voltage waveforms to give greater velocity to the tail of the ion bunch relative to the head.

Before embarking on construction of HTE, it was considered prudent to design and build a Multiple Beam Experiment (MBE) which would simulate in a pilot apparatus at a smaller scale as many as possible of the innovative accelerator features that are contemplated for HTE. The goal of MBE is to more fully establish the credibility of the HTE design concepts.

Until June 1984, the MBE effort was directed towards a sixteen-beam configuration (MBE-16) with injection at 2 MeV. The MBE-16 experiment would have been the bulk of the accelerator research to prepare the way for the High Temperature Experiment and was intended to address simultaneously both the beam physics of accelerating 16 beams to modest energy as well as demonstrating technology components at a scale suitable for HTE. This configuration was presented at the June 1984 DOE Review at LBL and is set forth in a separate report.⁽³⁾

In mid-July 1984, it was learned that the Senate/House Conference Committee had reduced the 9M\$ recommended in the President's Budget and by the House Appropriations Committee for the U.S. HIFAR program in FY85 to 5.5M\$. It was immediately clear that the MBE-16 plan as presented could not proceed in FY85 because that plan called for significant expansion in the engineering design effort and substantial front-end costs for tooling of the

focussing-arrays, large induction cores and large insulators. Consequently, the HIFAR group's effort switched to re-defining the program plan to be consistent with the FY85 budget. This resulted in the following plan for FY85 and beyond:

- 1) Proceed as rapidly as possible with a scaled-down Multiple Beam Experiment (called MBE-4, reflecting the choice of 4 beams) to constitute a proof-of-principle accelerator which can produce some results in FY85 and significant results in FY86. MBE-4 is described further in the following sections of this report.
- 2) Maintain the 2 MeV, 16-beam, high-current injector program at LANL in its present form as a technology development demonstration for HTE, but with a slip in schedule to late FY86. Postpone fabrication of the 16-beam matching/diagnostics section until FY86.
- 3) Postpone the development, fabrication and testing of large 16-beam HTE-size accelerating units until FY86 and FY87. In FY85, small-scale component development will continue, but at a modest pace.
- 4) Continue experiments with the Single Beam Transport Experiment (SBTE) until the end of FY85.

The foregoing plan should put us in a position in FY87 in which most of the novel physics of HTE will have been demonstrated at reduced scale on MBE-4 and in which many of the large-scale components for HTE (16-beam injector, matching/diagnostics section plus some accelerating /transport) will have been proven. Thus, one may then be in a position to proceed with confidence to build HTE.

The remainder of this report describes the anticipated performance and the major components of the MBE-4 Multiple Beam Experiment. The experimental program using this MBE-4 is described later together with a discussion of the physics and engineering issues which MBE-4 will be able to address.

B. MBE-4 PRINCIPAL PERFORMANCE PARAMETERS

The principal performance parameters for MBE-4 are set forth in Table B-1 together with the corresponding values for MBE-16 and the reference HTE design for comparison. We note the following with respect to Table B-1:

- 1) The beam-to-beam spacing (and therefore, the electrode-to-electrode pitch) are the same as were planned for MBE-16 and the ion beam transverse dimensions are comparable to those of MBE-16. Consideration was given to decreasing the transverse dimensions of the focussing arrays, but this was not done because it would have led to reduced line charge density, λ , which would have foreclosed exploring longitudinal strong-space-charge effects foreseen for HTE.
- 2) It should be noted that MBE-4 will be capable of demonstrating significant energy amplification (x4.5), current amplification (x4) and hence, power amplification (x18) towards that required for HTE (Ex60, Ix20).
- 3) The accelerating voltage impulses in MBE-4 are relatively large because of the lower injection energy. Thus, effects which might be seen in MBE-4 will be exaggerated compared to HTE which should facilitate observation and understanding of the phenomena.
- 4) Voltage "ears" will be applied to the head and tail of the bunch to limit bunch lengthening.
- 5) The last entry, $1 - (\sigma/\sigma_0)^2$, is the ratio of the space charge defocussing force to the mean restoring force. In all three cases it is close to unity, implying that all of the ion beams are heavily space-charge dominated.

TABLE B-1

PRINCIPAL PARAMETERS OF MBE-4 MULTIPLE BEAM EXPERIMENT WITH
CORRESPONDING VALUES FOR MBE-16 AND HTE INCLUDED FOR COMPARISON.

<u>Parameter</u>	<u>MBE-4</u>	<u>MBE-16</u>	<u>HTE</u>
Number of beams	4	16	16
Injection energy (MeV)	0.2	2	2
Ion (Charge +1)	Cs	Na(Cs)	Na
Injection current/beam (mA)	5-10	150(300 max)	300
Final current/beam (mA)	20-40	300(600)	6,000
Lattice 1/2-period (m)	0.23	0.32	> 0.3(varies)
Peak gap voltage (kV)	33	250	250
Accelerating gaps	24	25	~ 500
Cores/gap, max	~ 8	14	-
Length (m)	16	20	450
Length/Injected pulse length	12	< 3.5(8)	18
Final energy (variable) (MV)	0.5-1	< 8	125
Perveance (K_0) Injection:	4.2×10^{-4}	1.7×10^{-4}	3×10^{-4}
per beam Final:	1.2×10^{-4}	4×10^{-5}	1.3×10^{-5}
Minimum value of:			
$\frac{\omega_p^2}{2\omega_0^2} = (1 - (\sigma/\sigma_0)^2)$	0.94	0.94	0.98

C. MBE-4 General Arrangement

This and succeeding chapters give a technical description of the MBE-4 apparatus. These are followed by a description of the phased schedule for construction, installation and test such that experiments can be done with the early part of MBE-4 while the rest of MBE-4 is being built. The budget restraints mentioned earlier dictate that MBE-4 incorporate existing apparatus and components to a large degree and also dictate that the components be kept as simple and inexpensive as is consistent with meeting the basic objectives.

The MBE-4 Multiple Beam Experiment will be located in the existing Building 58 Hi-Bay as shown in Figures C-1 and C-2. The existing large 1 ampere Cesium Source and associated Marx generator^(6,7) which operate reliably at 200 to 400 kV will be converted to four small Pierce sources with alumino-silicate emitter buttons as described further in Section D2. This will be followed by a Beam Conditioning Unit consisting of four quadrupole doublets interspersed with diagnostic boxes and a vacuum isolation valve. The foregoing forms the Injector System of MBE-4.

Following the Injector System is the Accelerator Apparatus which comprises six Accelerator Sections each consisting of five quadrupole doublets interspersed with four accelerating gaps and associated induction cores for acceleration. A beam sensing box is located at the exit of each Accelerator Section. An energy analyzer can be placed after the final beam sensing box. The foregoing arrangement is shown diagrammatically in Figure C-3 and is shown in more detail in Figure C-4 and subsequent figures. Control and monitoring of MBE-4 will be performed at the control racks alongside of MBE-4, making a convenient arrangement for the experimenters. The Accelerator Apparatus is developmental because one of the main purposes of the experiment is to learn what induction waveforms are suitable and how to obtain them with arrangements of induction cores and pulser circuitry.

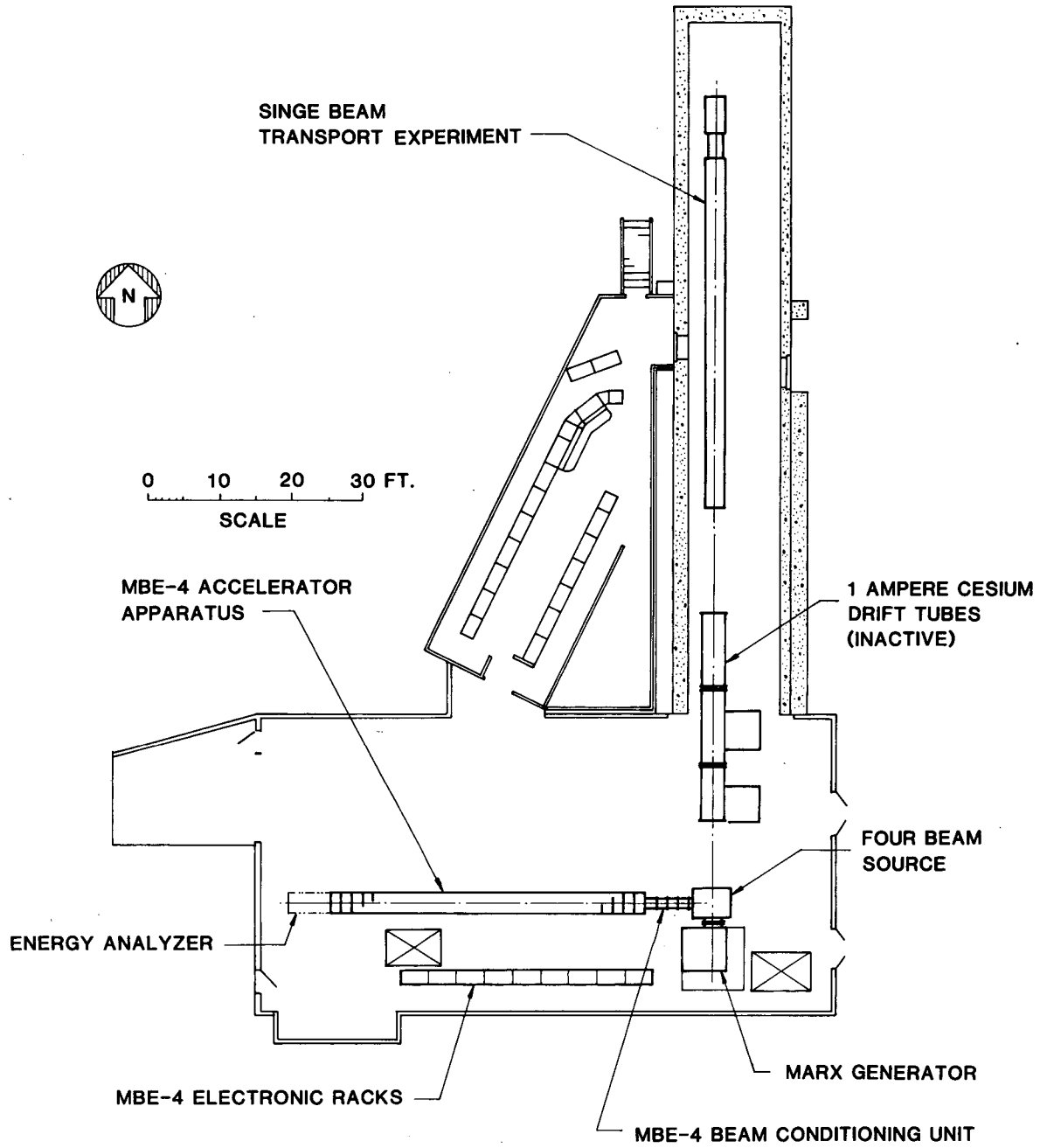
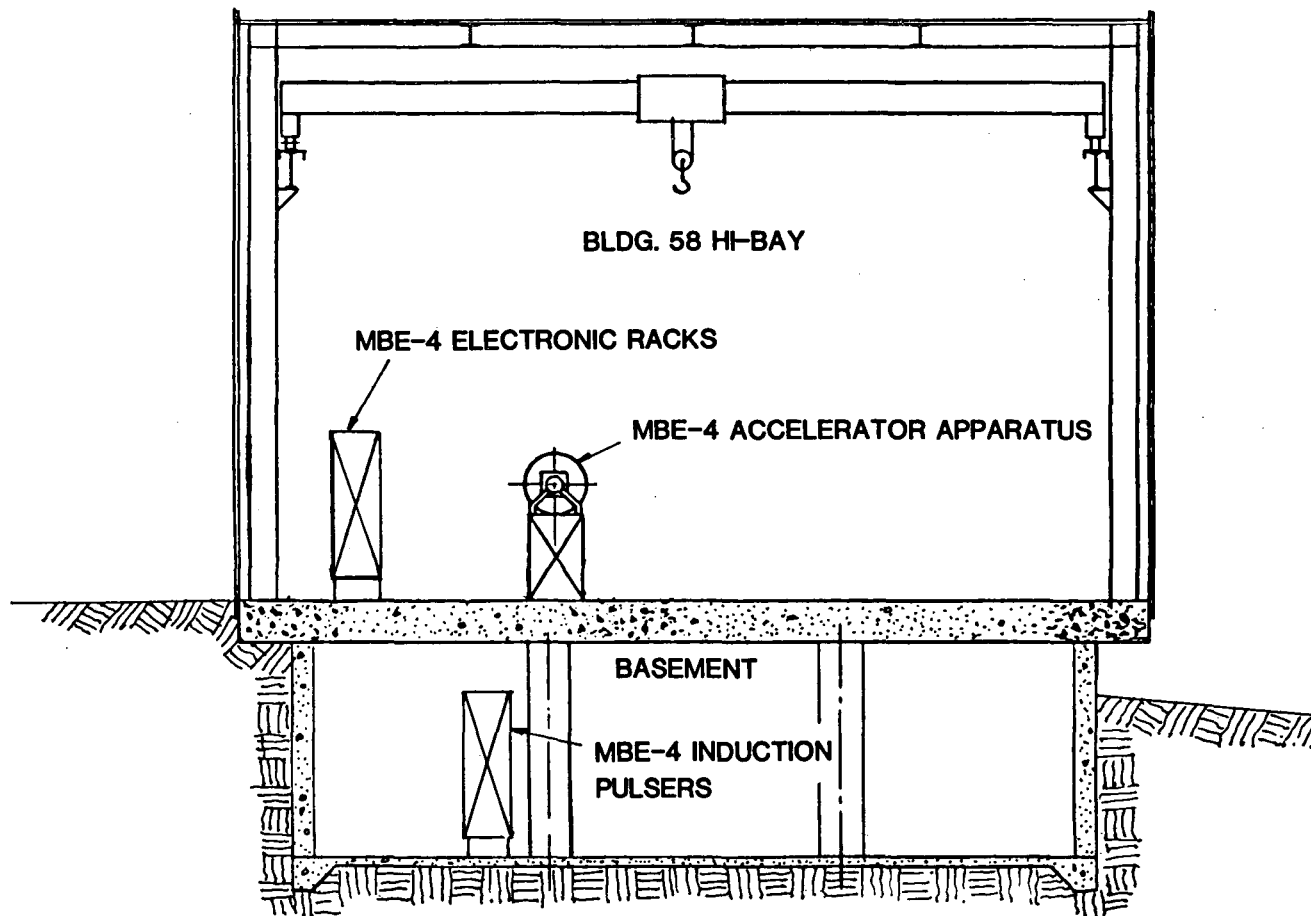


FIG. C-1

PLAN VIEW SHOWING MBE-4 LOCATED IN EXISTING BUILDING 58.

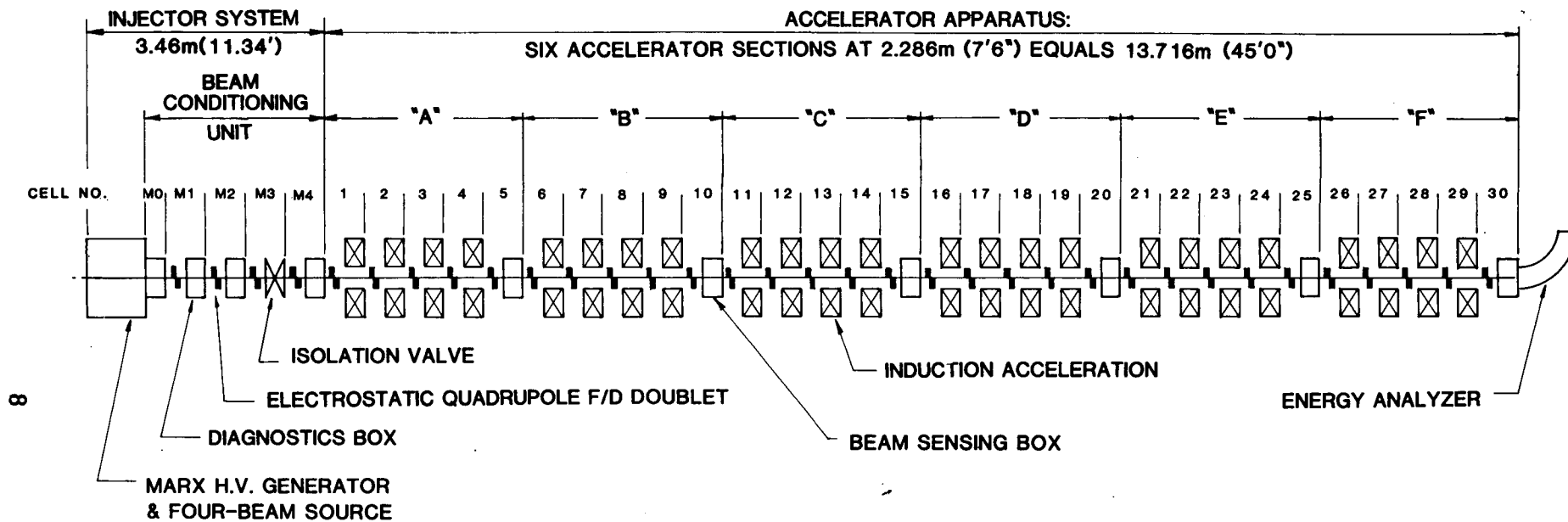
XBL 854-2075



CROSS-SECTION OF BUILDING 58 HI-BAY LOOKING WEST
SHOWING LOCATION OF MBE-4

FIG. C-2

XBL 854-2076



MBE-4
 DIAGRAMMATIC LAYOUT

FIG. C-3

MEASUREMENTS OF STABILITY LIMITS FOR A SPACE-CHARGE-DOMINATED ION BEAM IN A LONG A.G. TRANSPORT CHANNEL*

M. G. Tiefenback and D. Keefe
Lawrence Berkeley Laboratory
University of California
Berkeley, CA 94720

Abstract

The Single Beam Transport Experiment at LBL consists of 82 electrostatic quadrupole lenses arranged in a FODO lattice. Five further lenses provide a matched beam from a high-current high-brightness cesium source for injection into the FODO channel. We call the transport conditions stable if both the emittance and current remain unchanged between the beginning and end of the channel, and unstable if either the emittance grows or the current decreases because of collective effects. We have explored the range of single-particle betatron phase advance per period from $\sigma_0 = 45^\circ$ to 150° to determine the stability limits for the space-charge depressed phase advance, σ . No lower limit for σ (down to 7°) has been found at $\sigma_0 = 60^\circ$, whereas limits have clearly been identified and mapped in the region of σ_0 above 90° .

Introduction

Our practical motivation for the experiments reported here is the possibility of driving inertial confinement fusion via a heavy ion linear induction accelerator. In such a device, efficient acceleration requires very high beam current. For the fusion application, both transverse and longitudinal emittance must be kept very small to allow focussing of the beam onto the fusion fuel target. This experiment was designed to investigate the transverse stability limits of a beam in an A.G. lattice for high current and low emittance.

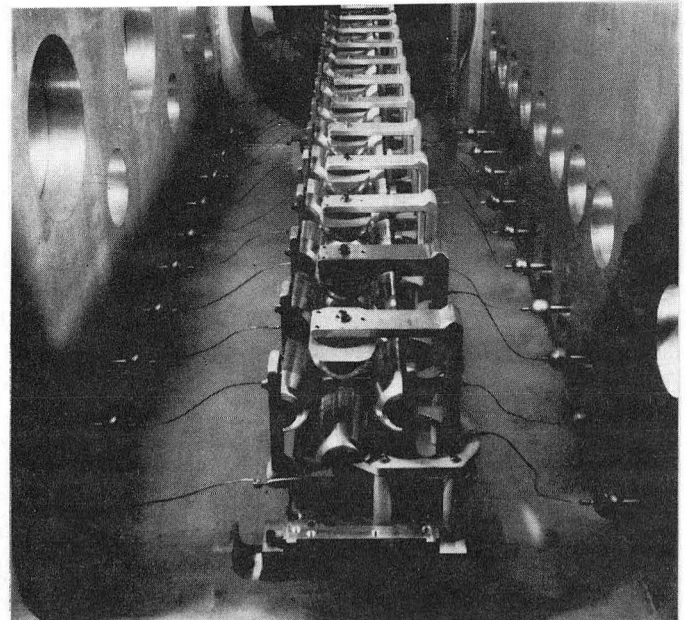
Apparatus

The Single Beam Transport Experiment (SBTE) comprises five matching quadrupoles (M1-M5) with independent voltage controls, followed by 82 quadrupoles (Q1-Q82) with equal voltages alternating in sign to form a long FODO transport lattice [1]. The quadrupole aperture is 25.4 mm in radius. A portion of the SBTE transport lattice is shown in Fig. 1 below. Cesium ions are produced from a heated aluminosilicate button 12.5 mm in radius, and are accelerated through a four-electrode injector to an energy that could be varied from 120 to 200 kV. Downstream of the injector a set of three biased grids could be introduced to increase the emittance, as desired, in a controlled way. Also at this location, a set of attenuators mounted on a large rotating wheel provides the capability of selecting a beam current with various values down to 1% of the unattenuated value. Two deep Faraday cups, each with a biased ring electrode (but no grid) at its entrance, could be introduced after M5 and after Q82 to give an absolute measurement of beam current at the beginning and end of the transport lattice. Additional current monitors - gridded Faraday cups that were shallow enough to slide between adjacent quadrupoles - were available for use at Q36 and Q60. Emittance measurements in both the (x,x') and (y,y') planes could be made by scanning with pairs of displaced slit-apertures at Q4-5, Q35-36, Q59-60, and Q80-81.

Experimental Method

The experimental procedure is straightforward. A value of σ is chosen by selecting the appropriate voltage for

Q1-Q82. The desired current and emittance are set by choice of the attenuator and the voltage applied to the emittance-spoiling control grids. With guidance from numerical integration of the Kapchinskij-Vladimirskij (K-V) envelope equations, the voltages of the matching quadrupoles M1-M5 are tuned until the emittance ellipses in (x,x') and (y,y') phase-space have the correct size and orientation to deliver a matched beam to the transport system. (A beam is considered "well-matched" if the residual envelope oscillation amplitude is less than $\pm 10\%$ of the beam radius.) If the current and emittance are found to be unchanged in passing through the entire transport system, it is empirically labeled as "stable". If either has changed, however, the additional diagnostics at Q35 and Q59 are activated to provide more information on the evolution of the unstable behavior.



CBB 831-845

Fig.1. A portion of the SBTE transport lattice

Results

The quantities σ_0 and σ are, resp., the betatron phase advance of a particle in the lattice with and without space-charge. Measurements were made for 13 values of σ_0 from 45° to 150° . Given the uniformly placid behavior of the beam observed for $60^\circ \leq \sigma_0 < 85^\circ$, we made only one brief measurement for $\sigma_0 = 45^\circ$ and none for $\sigma_0 < 45^\circ$. For $\sigma_0 > 120^\circ$, the closed orbit deviations due to misalignments become large, precluding meaningful measurements for $\sigma_0 > 150^\circ$.

In summary, beam behavior was always found to be stable below $\sigma_0 = 90^\circ$ within the limits of current and emittance accessible to us, and unstable above $\sigma_0 = 90^\circ$ if a sufficiently high current was injected.

*This work was supported by the Office of Energy Research, Office of Basic Energy Sciences, U.S. Department of Energy under Contract No. DE-AC03-76SF00098.

The emittance at injection into the periodic lattice began to increase above the baseline value for $\sigma_0 = 85^\circ$ rather than $\sigma_0 = 90^\circ$, but we attribute this to aberrations from the matching section, which became visibly more pronounced as we attempted to match into stronger lattices. This might also be due to exceeding the stability limits locally in the matching section, as the beam disruption at even slightly higher σ_0 is very rapid.

Figures 2 and 3 are representative of how differently the beam acts depending on whether σ_0 is less than or greater than 90° . To obtain these graphs, we have chosen contours of equal density in the measured (x, x') distribution and have displayed the total inscribed current versus the phase-area (divided by π) within the contour. We have chosen to estimate this phase area by calculating the root-mean square emittance of the (x, x') distribution within the contour, and then multiplying by $4\beta\gamma$ to give a corresponding normalized K-V emittance. Thus

$$\epsilon = 4\beta\gamma (\langle x^2 \rangle \langle x'^2 \rangle - \langle x x' \rangle^2)^{1/2},$$

with x and x' measured from the centroid of the figure. This definition of area/π is not far from the circumscribed area/π as directly measured, but is more stable against fluctuations in the data, and is of use in estimating σ as described below.

The $[\epsilon, I(\epsilon)]$ presentation was chosen because it graphically displays the ratio ϵ/I , which is of great importance in parameterizing the depressed tune. We will illustrate a scaling possible in a linear lattice via an envelope equation, but the basic idea holds for general Vlasov equilibria by scaling the distribution function. Consider the smooth approximation envelope equation for a K-V distribution:

$$a'' + Ka - \frac{Q}{a} - \frac{\epsilon^2}{a^3} = 0.$$

While maintaining the same beam dynamics, including (σ_0, σ) , we may re-scale the radius $a \rightarrow ka$, and scale $Q \rightarrow k^2 Q$ and $\epsilon \rightarrow k \epsilon$. The envelope equation is satisfied, and the ratio ϵ/I is the same as for the original solution. It is this ratio, in general, that determines the σ , given σ_0 . The real brightness, proportional to I/ϵ^2 , is not the determining parameter. It is true that for real beams σ is not uniform for all particles, but we make contact with the RMS

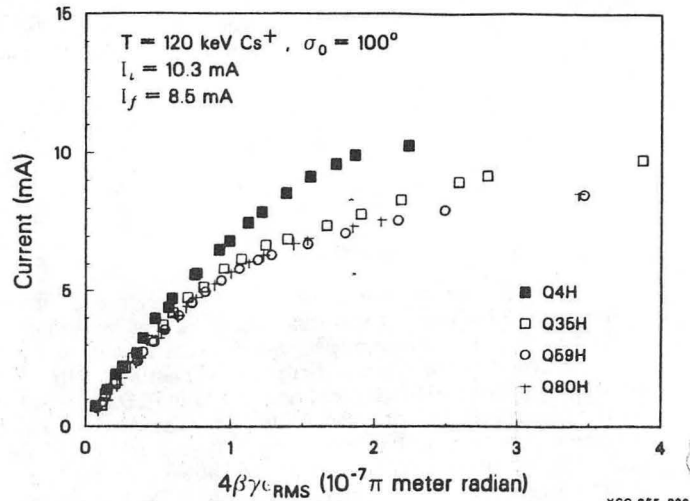


Fig. 3. Data obtained as for Fig. 2., but current drops as emittance initially rises. Collective effects drive particles from the core of the distribution and cause beam loss until apparently stable asymptotic distribution forms.

envelope equations by noting that with the RMS emittance constant, the K-V equations are identical in form to the RMS equations [2]. We then use the K-V equivalent σ as a measure of beam intensity, some average of all particles' oscillation frequencies.

We define two slightly different quantities σ and σ' according to the following recipe. The three measured quantities are ϵ , $I(\epsilon)$, and the beam radius at a point of antisymmetry; inserting ϵ and $I(\epsilon)$ into the K-V equations allows one to derive a phase advance per period for a single particle moving in the combined fields (both assumed linear) of the space-charge and quadrupole forces. Inserting the full beam values (ϵ_0, I_0) into the K-V equations, we derive a value σ for the depressed tune. Using the core 95% of beam current to calculate ϵ' , the emittance of this sub-distribution, we calculate σ' from $(\epsilon', .95 \times I_0)$. The values are typically close to each other, but the difference is a measure of the extent of the halo of the beam in phase space. In practice, we have found that the radius derived using (ϵ, I) is in very close agreement with the measured value. Because the 95% emittance was more immune to fluctuations in value from run to run, emittances quoted in the following text will be 95% core values. (The intuitive value of thinking of σ in terms of defining a smoothed slow sinusoidal motion of a single particle may become of questionable value, however, when the space charge and average external fields are virtually cancelling each other. In that case, the nonlinear forces can predominate in determining the particle motion.)

The Region $\sigma_0 < 90^\circ$

To obtain the lowest possible value of σ , the emittance grids were removed to minimize the emittance. Figure 1 shows the results for one example run $\sigma_0 = 60^\circ$ and $\sigma = 8^\circ$. The emittance distribution can be seen to be unchanged, as measured at several points throughout the transport system. The behavior is the same for all other values of σ_0 less than 85° for the same injected beam emittance and current. At such low σ values, the emittance term in the envelope equation is very small compared with the space-charge term.

For a K-V distribution, the graph of I vs. ϵ is a straight line segment; the data have close to a linear form, too, except for the contribution from the tails of the

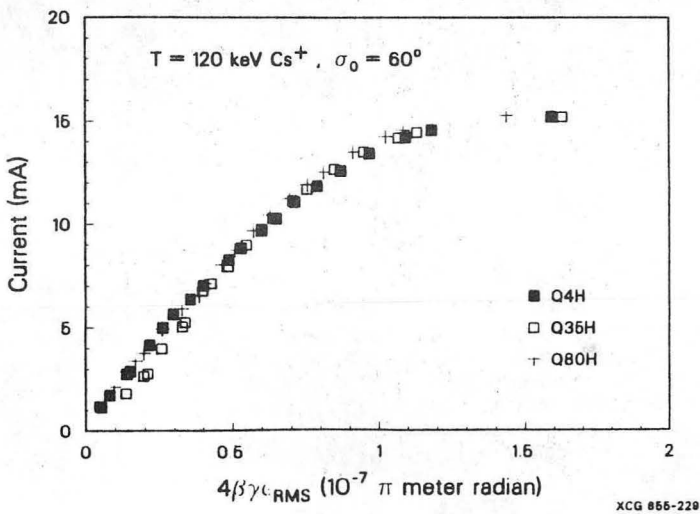


Fig. 2. From the measured (x, x') distribution of the beam at various lattice locations we calculate the RMS emittance and enclosed current of sub-distributions bounded by various intensity contours. Beam current is 15.2 mA, and emittance is well maintained through the lattice.

distribution. In reality, the actual beam is not well represented by a K-V distribution; while it is approximately uniform in configuration space, it has a nearly Gaussian distribution in transverse velocity. (We refer to this as "semi-Gaussian".) For beams with significantly lower current or larger emittance, when the emittance term in the envelope equation is not negligible, the data points lie to the right of the curve shown and tend to be convex upwards.

The Region $\sigma_0 > 90^\circ$

In all cases studied, unstable beam behavior could be observed and the properties of the injected beam did not set a limitation. For $\sigma_0 \geq 120^\circ$, characterization of the beam limits was straightforward. We found that too low a value of σ at injection resulted in a degraded, higher value at Q80. As we raised the ϵ/I of the injected beam, the output ϵ/I fell until the two coincided, then both rose together. For cases in which the current and emittance were preserved over the full lattice, the data are plotted in the summary Figure 4 with filled-in symbols.

Figure 3 illustrates beam evolution for one case, for $\sigma_0 = 100^\circ$, injection current of 10.3 mA, and 95% emittance $1.8 \times 10^{-7} \pi$ meter radian. In the 10% periods between Q4 and Q35 the beam evolves significantly, with somewhat more change occurring by Q59. No change is detectable afterward to Q80.

Injection for these current and emittance values was chosen because an earlier 15 mA, $1.4 \times 10^{-7} \pi$ emittance beam showed this same pattern, degrading to 10 mA with emittance $2.2 \times 10^{-7} \pi$ at Q59, but seemingly stable with those parameters from then on to Q80. For $\sigma_0 = 100^\circ$ we have plotted the optimal results from initially unstable conditions for which the beam showed no change from Q59 to Q80. The same is true for the 93° and 97° lattice. We plan further investigation in the region $90^\circ < \sigma_0 < 120^\circ$.

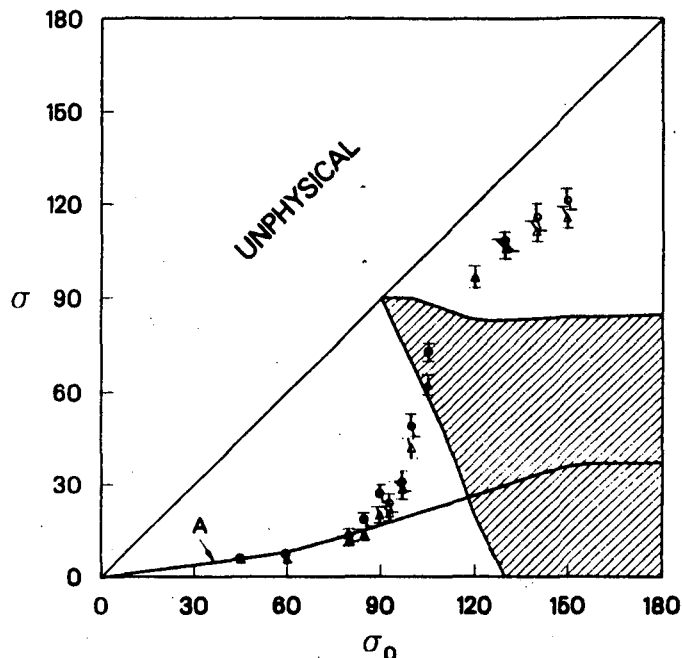
While the data analysis is not complete and a theoretical basis for understanding not yet in hand, we report these preliminary results as well-documented experimental data. The spontaneously organized, apparently stable asymptotic 10 mA distribution observed for $\sigma_0 = 100^\circ$ appears to allow for more current at a lower emittance than does the semi-Gaussian distribution with the same current and RMS emittance that we can obtain directly from our source. One cannot, of course, be certain that evolution to a truly stable distribution (i.e., with exact current and emittance conservation) is being observed or whether emittance growth is still proceeding but at an undetectably low rate.

Discussion of Results

Figure 4 shows a summary of results to date. Source properties set limits on how small a value for σ/σ_0 can be explored. Below $\sigma_0 = 90^\circ$, and for strongly depressed betatron frequency, σ varies as $\sigma_0^2(\epsilon/I)$ and so is limited by the transverse temperature and the emission of the source. It has been found that the lowest values of σ can be explored if we operate the injector in a high perveance configuration, limited to 120 kV by sparking.

For $\sigma_0 < 85^\circ$, the data points represent the lowest values of σ reached; in all cases, beam propagation was found to be stable and well represented by the data in Fig. 2. How much further down in σ the beams remain stable is not known; simulations suggest that the limit will be set by nonlinearities due to the vacuum field and due to image charges when the effects of misalignment are taken into account [3].

In the right hand part of the diagram are plotted the values of σ corresponding to the values of emittance



XCG 856-233

Fig. 4. Plotted are calculated σ values for stable and apparently stable beams for various σ_0 . Filled-in symbols represent beams with the same current and emittance at the beginning and end of the lattice. Hollow symbols mark σ values derived from beams reproducing ϵ and current over at least the last 10 periods, as illustrated in Fig. 3 for $\sigma_0 = 100^\circ$. Circles mark σ values derived using full beam distribution RMS emittance. Triangles mark calculations using central 95% current of the phase space distribution. The shaded region marks the calculated instability of the envelope equations. Curve A marks the region of equivalent σ attainable at injection with our limited source emittance.

and current representing stable propagation through the full SBTE lattice or asymptotically stable propagation through at least the last 10 periods, as for the example of Figure 3.

More data points can be added below $\sigma_0 = 45^\circ$ by stopping down the radius of the beam; it has not been thought urgent to do so because such weak focussing seems inapplicable to practical accelerator applications, and no different physics is expected.

References

- [1] A. Faltens, D. Keefe, C. Kim, S. Rosenblum, M. Tiefenback, A. Warwick, Proc. 1984 Lin. Acc. Conf. (Seeheim), GSI-84-11, 312 (1984).
- [2] F. J. Sacherer, Proc. 1971 Part. Acc. Conf., IEEE Trans. Nuc. Sci., NS-18 (3), 1105-1107.
- [3] C. Celata, I. Haber, L. J. Laslett, L. Smith, and M. G. Tiefenback, elsewhere in this conference.

This report was done with support from the Department of Energy. Any conclusions or opinions expressed in this report represent solely those of the author(s) and not necessarily those of The Regents of the University of California, the Lawrence Berkeley Laboratory or the Department of Energy.

Reference to a company or product name does not imply approval or recommendation of the product by the University of California or the U.S. Department of Energy to the exclusion of others that may be suitable.

*LAWRENCE BERKELEY LABORATORY
TECHNICAL INFORMATION DEPARTMENT
UNIVERSITY OF CALIFORNIA
BERKELEY, CALIFORNIA 94720*